

Kinetics and Dose-Dependency of Intranasal Oxytocin Effects on Amygdala Reactivity

Franny B. Spengler, Johannes Schultz, Dirk Scheele, Maximiliane Essel, Wolfgang Maier, Markus Heinrichs, and René Hurlemann

Supplemental Information

Table of contents

1. <u>Supplemental Methods</u>	<u>2</u>
1.1. Ethics and enrollment	2
1.2. Participants	2
1.3. Screening session	2
1.4. Intranasal treatment	3
1.5. Neuroendocrine parameter extraction	3
1.6. Task conceptualization	4
1.7. Stimuli preparation and pilot study	4
1.8. fMRI task	6
1.9. Data analysis	7
2. <u>Supplemental Results</u>	<u>11</u>
2.1. Missing values	11
2.2. Demographical data, salivary and plasma OXT concentrations	11
2.3. Whole brain results	11
2.4. Amygdala results	12
2.5. Behavioral results	15
2.6. Autism quotient dependent results	18
2.7. Further moderation effects	18
2.8. Blinding of the treatment	19
3. <u>Supplemental Discussion</u>	<u>20</u>
3.1. Alternative explanations	20
3.2. Whole brain findings	20
3.3. Intranasal delivery route	20
4. <u>Supplemental Tables</u>	<u>22</u>
5. <u>Supplemental Figures</u>	<u>25</u>
6. <u>Supplemental References</u>	<u>31</u>
7. <u>CONSORT Checklist</u>	<u>34</u>
8. <u>CONSORT Flow Diagram</u>	<u>36</u>

SUPPLEMENTAL METHODS

Ethics and enrollment

The study was approved by the local ethics committee of the Medical Faculty of the University of Bonn, Germany. The study was registered in the Clinical Trials.gov database (Identifier: NCT03011970) provided by the US National Institutes of Health. All subjects gave written informed consent and the study was conducted in accordance with the latest revision of the Helsinki Declaration. Participants were recruited from the local population by means of newspaper announcements, public postings and flyers (recruitment period: December 2013 – December 2014). After completion of the study, subjects received monetary compensation.

Participants

Out of 133 participants invited to the screening appointment (exclusively non-smoking right-handed men, aged 18 to 40 years), 17 were not eligible for enrollment (for exclusion criteria, see **Screening session**). Thus, the final sample comprised 116 healthy male subjects (mean age \pm SD: 24.7 \pm 4.4 years), which were randomly assigned to five treatment conditions exemplified below.

Screening session

Enrollment was preceded by a screening appointment which ensured that all subjects were free of any current or past physical or psychiatric illness as assessed by medical history and the Mini-International Neuropsychiatric Interview (MINI) (1). We additionally confirmed that subjects were naive to prescription-strength psychoactive medication and had not taken any over-the-counter psychoactive medication in the preceding four weeks. To further characterize the sample, we acquired sociodemographic data and neuropsychological questionnaires of each participant. In particular, we assessed trait anxiety (State-Trait Anxiety Inventory, STAI) (2), depressive symptoms

(Beck Depression Inventory, BDI-II) (3), alexithymia symptoms (Toronto Alexithymia Scale, TAS) (4) and autistic-like traits (Autism-Spectrum Quotient, AQ) (5).

Intranasal treatment (additional information)

Participants self-administered 12, 24 or 48 IU synthetic oxytocin (OXT) (depending on the treatment group) and placebo (PLC) via nasal spray at the beginning of each testing sessions (i.e. 3, 6 or 12 puffs balanced across nostrils, at an inter-puff interval of 50 seconds to allow the solution to be absorbed into the nasal epithelium). The amount of administered substance was weighed, and if falling below a set minimum (24 IU = 600 mg, 12 IU = 300 mg, 48 IU = 1200 mg), supplemented by an additional puff. After each session, participants were asked to guess whether they had received PLC or OXT.

Neuroendocrine parameter extraction

Saliva samples were collected using commercial sampling devices (Salivettes, Sarstedt, Germany) which were immediately centrifuged at 4000 rpm for 2 min and stored at -80°C until assayed. Plasma samples were collected with commercial sampling devices (Vacuette, Greiner Bio-One International, Austria) containing EDTA and aprotinin. Vacuettes were immediately centrifuged at 3250 rpm for 10 min, and aliquoted samples were stored at -80°C until assayed. OXT concentrations were extracted and quantified using a highly sensitive and specific radioimmunoassay (RIAgnosis, Munich, Germany) (6). The limit of detection was 0.1 - 0.5 pg, depending on the age of the tracer. Intra-assay and inter-assay coefficients of variability were < 10 %. All samples to be compared were assayed in the same batch, i.e. under intra-assay conditions.

Task conceptualization

The conceptualization of our task was based mainly on previous findings from a recent meta-analysis (7), which summarized data from studies exclusively examining OXT's effect on recognition accuracy of full-face, basic expressions of emotion. Moreover, Shahrestani and colleagues compared OXT's influence on the processing of various emotional expressions (happy, sad, angry, fearful, surprised and disgusted). The authors concluded that OXT significantly enhances the recognition accuracy of happy and fearful facial expressions. We thus decided to use facial expressions of happiness and fear, to increase the likelihood of obtaining OXT-modulated responses. We further decided to vary the intensity of the emotional expressions to avoid obscuring OXT responses due to ceiling effects in the behavioral performance and therefore included low saliency emotional stimuli at 35 % emotional intensity. However, to guarantee a reasonable amygdala response, we also included highly salient emotional stimuli at 65 % emotional intensity.

Stimulus preparation and pilot study

Face pictures used in the facial emotion recognition task displayed neutral mood, high and low intensity fear, as well as high and low intensity happiness. Stimuli were morphed into increasingly intense emotional expressions (see **Morphing procedure**). The final stimulus pool was chosen based on a comprehensive pilot study (see **Pilot study**).

Morphing procedure

All stimuli were created based on standardized face pictures from the 'Karolinska Directed Emotional Faces Battery' (KDEF (8)). We selected neutral, fully happy and fully fearful facial expressions from 25

male and 25 female actors from the KDEF¹. These pictures served as source pictures for the morphing process. Using the software 'Abrosoft FantaMorph 5' (Abrosoft, Beijing, China), we created increasingly fearful and increasingly happy faces of each actor in increments of 5 % change by interpolating (morphing) the individual photo of the neutral facial expression into the individual fearful and happy facial expression, respectively. Approximately 100 points were set on corresponding spots of the faces (e.g. eyes, mouth, nose, chin, forehead, hair) to create a fine-grained transition from one face to another. This procedure resulted in two series of 20 emotional pictures with increasing emotional intensity of happiness and fear for each actor (for an example see **Supplemental Fig. S1**).

Pilot study

To verify the morphing procedure and to identify perceptual thresholds of emotion recognition, we conducted a behavioral pilot study on an independent sample of 40 healthy subjects which were not enrolled in the main study. The face stimuli were presented on a computer screen for 3 seconds using the presentation software Presentation (NeuroBehavioral Systems, Inc., Berkeley, CA, USA). Each subject was presented with a selection (360 pictures) of the whole stimulus set (50 actors x 20 facial expressions of increasing fear (2000 stimuli) and happiness (2000 stimuli)) and instructed to indicate whether they perceived the depicted face as neutral, fearful or happy (same task as in the main study). A randomization algorithm ensured that each single picture was rated by at least three different subjects.

¹ KDEF stimuli used in Set A: F1, F3, F5, F8, F9, F11, F12, F13, F17, F18, F19, F29, M1, M2, M3, M4, M6, M9, M10, M11, M12, M13, M14, M17, M23.

KDEF stimuli used in Set B: F2, F22, F23, F25, F26, F27, F28, F30, F31, F32, F33, F34, F35, M2, M7, M18, M22, M24, M25, M27, M28, M29, M30, M34, M35.

Mean results across facial pictures of all actors are depicted in **Supplemental Fig. S2**. As expected, recognition rate increased steadily with the facial expressions' emotional intensity. At 40 % intensity, half of the subjects recognized the target emotion correctly (i.e. as happy and fearful, respectively), while the other half still experienced the expression as neutral. Emotional expressions of 65% intensity were classified as emotional by over 90 % of the subjects and were thus chosen as 'high intensity' stimuli for the main experiment. Emotional expressions of 35 % intensity were classified as emotional by less than half of the subjects and thus chosen as 'low intensity' stimuli for the main experiment.

fMRI task

Stimuli comprised morphed face pictures displaying neutral mood and high and low intensity fear and happiness (see **Fig 1**). Neutral mood pictures were displayed twice to balance the number of pictures of each intensity. To avoid stimulus repetition effects, the 300 stimuli were divided into two sets presented in a counterbalanced order across sessions.

The fMRI scan consisted of an event-related facial emotion recognition paradigm. In each trial, a stimulus was presented for 3 s followed by a jittered inter-stimulus interval (4-6 s, mean = 5 s) during which a fixation cross was presented. Stimuli were presented through MRI-compatible goggles using the software Presentation (Neurobehavioral Systems Inc., Berkeley, CA, USA). Participants were instructed to identify the emotion depicted by the face in the picture (neutral mood, happiness or fear) as quickly and accurately as possible by pressing one of three buttons on an MRI-compatible response grip system (NordicNeuroLab AS, Bergen, Norway). Participants learned the button press coding before the scan. Trials were split into two consecutive runs (11.5 min each) to allow participants a short rest; total scanning time was 23 min per session.

Data analysis

Behavioral data analysis

Quantitative behavioral data were compared by repeated measures analysis of variance (ANOVA). The assumption of sphericity was assessed with Mauchly's test, and for significant violations, Greenhouse-Geisser's correction was applied. Post hoc analyses to delineate higher order effects were calculated using paired t-tests. Pearson's product-moment correlation was used for correlation analysis. Eta-squared and Cohen's d were calculated as measures of effect size. For qualitative variables, Pearson's chi-squared tests were used. Two-tailed P-values of $P < .05$ were considered significant.

Acquisition of functional MRI data

The MRI data were collected using a 1.5-tesla Siemens Avanto MRI system (Siemens AG, Erlangen, Germany). T2*-weighted echoplanar (EPI) images with blood-oxygen-level-dependent contrast were obtained [repetition time (TR) = 3000 ms, echo time (TE) = 50 ms, interleaved slicing, matrix size: 64 x 64, voxel size: 3.3 x 3.3 x 3 mm, distance factor = 10 %, flip angle 90°, 35 axial slices] using an amygdala sensitive sequence, optimized as follows: To refine imaging in subcortical regions, TE was decreased linearly by 10 ms in a transition zone between slice 19 and slice 14, resulting in a final TE of 40 ms in the lower slices, as previous studies have shown largest amygdala activations at an echo time of 40 ms (9). In addition, high-resolution anatomical images were acquired on the same scanner using a T1-weighted 3D MPRAGE sequence (imaging parameters: TR = 1660 ms, TE = 3.09 ms, matrix size: 256x256, voxel size: 1 x 1 x 1 mm, flip angle 15°, 160 sagittal slices).

Preprocessing

We discarded the first five volumes of each functional time series to allow for T1 signal equilibration. Images were corrected for head movement between scans by an affine registration. Six subjects with substantial head movements (> 3 mm in any dimension) were excluded from further analysis, as adequate correction could not be guaranteed. Images were initially realigned to the first image of the time-series and then re-realigned to the mean of all images. For spatial normalization, the mean EPI image of each subject was normalized to the current Montreal Neurological Institute (MNI) template (10, 11) using the unified segmentation function in SPM8. All images were transformed into standard stereotaxic space and resampled at 2 mm x 2 mm x 2 mm voxel size. The normalized images were spatially smoothed using an 8-mm full width at half maximum Gaussian kernel. Raw time series were detrended by the application of a high-pass filter (cutoff period, 128 s).

fMRI data analysis

Functional data were analyzed using a two-stage approach based on the general linear model implemented in SPM8: individual participants' data were modeled with a fixed-effect model, and their summary data were analyzed at the group level using a random effects model. In the fixed-effects model, the five conditions of each session (neutral, low fearful, high fearful, low happy, high happy faces) were modeled by a stick function and convolved with a hemodynamic response function (HRF (11)). Button presses were modeled as regressors of no interest. Movement parameters estimated during motion correction were included as confound regressors. Linear contrasts were applied to the individual parameter estimates of the response to the experimental conditions, resulting in contrast images. First, each emotional condition was compared to the neutral face condition for the OXT and PLC session separately (i.e. [low fear – neutral faces], [high fear – neutral faces], [low happy – neutral faces], [high happy – neutral faces]) and pooled across emotions (i.e. [fear – neutral faces], [happy – neutral faces]). Second, treatment effects on emotion-specific

responses were assessed (e.g. [(FearPLC > NeutralPLC) > (FearOXT > NeutralOXT)]; [(HappyPLC > NeutralPLC) > (HappyOXT > Neutral OXT)]).

To validate previous findings, the latter contrast images of fear-specific responses [(FearPLC > NeutralPLC) > (FearOXT > NeutralOXT)] were then subjected to a group-wise random effects ANOVA (significance threshold of $P < .05$, corrected for multiple comparisons [family-wise error (FWE)]) in the subsample having received 24 IU OXT 45 min prior to the fMRI task. A region of interest (ROI) analysis was conducted using the anatomically-defined bilateral amygdala masks provided in the WFU PickAtlas toolbox for SPM (<http://fmri.wfubmc.edu/software/pickatlas>) (12) at a threshold of $P < .05$ and FWE-corrected for multiple comparisons based on the size of the ROI. Indeed, we found significant deactivation in the left ($P = .046$) but not right ($P = .79$) amygdala when applying a region of interest analysis to this contrast. In a second step we were interested in how far this dampening effect in the left amygdala is moderated by fear intensity, and thus conducted a two-way ANOVA with the within-subject factors treatment (OXT, PLC) and intensity (neutral, low, high) and the parameter estimates averaged across all left amygdala voxels (PE_{AMY}) as dependent variable (results are reported in the main text). Since the main treatment effect of OXT on fear-specific activation did not reach significance in the right amygdala, we decided to focus on the left amygdala activation.

To specifically investigate dose- and latency-dependent responses in the left amygdala, we then extracted individual parameter estimates (PE_{AMY}) from the amygdala for all conditions using a custom MATLAB script, using the WFU PickAtlas amygdala mask (12). Selecting amygdala voxels of interest anatomically rather than through a contrast of parameter estimates from our dataset eliminates the so-called 'double-dipping' issue in fMRI statistics (13). These data were further analyzed in SPSS and subjected to repeated-measures ANOVAs and paired t-tests.

To examine whether autistic-like traits moderate fear processing, we conducted a regression analysis to predict whole brain PLC response to fearful faces based on the individual autism quotient (AQ).

Following on the amygdala findings under PLC described in the results section ('Autism Quotient – fMRI results'), we investigated whether AQ also moderated OXT effectiveness. AQ scores were used in regression analyses to predict the difference between the OXT and PLC sessions in the behavioral and fMRI data (PE_{AMY}) (14). As an additional moderator test, we median-dichotomized the AQ score (median split at AQ = 13.5) and conducted separate analyses in the high (n = 55) and low (n = 55) AQ groups.

SUPPLEMENTAL RESULTS

Missing values

Two saliva samples and seven plasma samples were lost due to problems in sample assessment or analysis. Behavioral data from eight subjects were not recorded in one fMRI session due to technical issues in the response grip system. The respective subjects were thus excluded from behavioral data analysis. MRI data from nine subjects had to be excluded due to considerable head movements (> 3 mm movement in any direction as assessed by SPM's realignment procedure, six subjects) or failures in data recording (three subjects).

Demographical data, salivary and plasma OXT concentrations

Treatment groups did not differ in demographical or neuropsychological measurements, and treatment had no effect on mood or state anxiety (see **Supplemental Table S1, S2**). OXT levels (see **Fig. 2**) did not differ between sessions at baseline (plasma: all P s > .34 for all dose groups; saliva: all P s > .30), but were significantly elevated following OXT compared to PLC treatment at all sampling time points (saliva and plasma: all P s < .01).

In all treatment groups saliva and plasma OXT concentrations were significantly increased after administration of OXT (AUC_i: all P s < .01; plasma concentrations: all P s < .01) but not after administration of PLC (AUC_i: all P s > .09; plasma concentrations: all P s > .12).

Whole brain effects

This study was specifically designed to investigate the effect of variations in OXT dose and administration latency on the amygdala response to emotional stimuli. Nevertheless, we briefly explored whole brain findings and obtained the following results. Processing of emotional faces

compared to neutral faces [Emotional_{PLC} > Neutral_{PLC}] elicited activations in a broad network of brain regions involving frontal, midcingulate and fusiform areas (cf. **Supplementary Table S3**). OXT enhanced the response to emotional stimuli [(Emotional_{OXT} > Neutral_{OXT}) > (Emotional_{PLC} > Neutral_{PLC})] in the insula bilaterally, in the right cingulate gyrus, right caudate and in the right superior frontal gyrus as well as the left precentral gyrus. Activation was decreased in the right superior temporal sulcus and the left medial frontal gyrus following OXT treatment (the threshold used was $P_{FWE} < .05$; cf. **Supplemental Table S4 and Fig S3** for details). When restricting the analyses to the amygdala (unilateral ROIs), neural activity decreased significantly after OXT treatment in the left (-20, -4, -20, $t_{(1,808)} = 3.43$, $k = 91$, $P_{FWE} = .025$) but not in the right amygdala. We then tested the dose- and latency effects obtained in the left amygdala in the whole brain, looking for variations as a function of dose and latency in the response measured in the following contrasts: [(High fear_{OXT} > Neutral_{OXT}) > (High fear_{PLC} > Neutral_{PLC})] and [(Low fear_{OXT} > Neutral_{OXT}) > (Low fear_{PLC} > Neutral_{PLC})]. We found no results that survived corrections for multiple comparisons across the whole brain

Amygdala results

Cytoarchitectonic mapping of amygdala subregions

OXT significantly reduced the response to fearful faces [(Fear_{PLC} > Neutral_{PLC}) > (Fear_{OXT} > Neutral_{OXT})] in an amygdala cluster ($k = 90$) with the two MNI peak coordinates x, y, z : -26, -6, -16 ($t_{(1,808)} = 3.47$, $P_{FWE} = .046$) and -18, 2, -16 ($t_{(1,808)} = 3.38$, $P_{FWE} = .051$). Using probabilistic cytoarchitectonic maps derived from human post-mortem studies, as integrated in the SPM Anatomy toolbox V1.8 (15), these two peak coordinates were mapped to the basolateral and superficial subregions of the amygdala, respectively. Probabilities for the assigned regions were as high as 80% and 90%, respectively. However, one has to take into account that our data were obtained on a 1.5T scanner, which yields data with much lower spatial resolution than what can be obtained at 3T or higher field

strengths. Hence, inferences about localization to particular subnuclei should be considered with caution and replicated at a higher magnetic field.

Amygdala response to emotional faces of varying intensity

Consistent with previous findings (16), emotional faces elicited higher amygdala BOLD responses than neutral faces in the PLC condition. A repeated-measures ANOVA with the within-subject factors hemisphere, type of emotion and emotion intensity revealed that BOLD response varied with the intensity of the face's emotional expressiveness (main effect of intensity: $F_{(1,105)} = 16.28$, $P < .001$, $\eta_p^2 = 0.13$), but not with the type of emotion, and did not vary across hemispheres (no further significant main effects or interactions). As expected, high intensity emotional faces induced stronger BOLD response increases than low intensity emotional faces ($t_{(105)} = 2.83$, $P < .01$, $d = 0.27$), which underlines the successful manipulation of emotional salience achieved by our stimulus set (see **Supplemental Fig. S4**).

Effect of oxytocin on the amygdala response to emotional stimuli

Next, we assessed the effects of OXT on the amygdala response. As previous studies indicated that these effects can be highly heterogeneous across hemispheres and emotions, we investigated whether OXT effects varied across left and right amygdala, and as a function of the face's emotion and emotional intensity (repeated-measures ANOVA with within-subject factors treatment, hemisphere, face emotion and emotion intensity, and between-subject factor subject group). We found a main effect of intensity ($F_{(1,101)} = 23.26$, $P < .01$, $\eta_p^2 = 0.19$) and an interaction between treatment and hemisphere ($F_{(1,101)} = 6.93$, $P = .01$, $\eta_p^2 = 0.06$). We thus proceeded to analyze the data of each hemisphere separately (same ANOVA as above, without the factor hemisphere). In the left

amygdala, we found main effects of treatment ($F_{(1,101)} = 3.98$, $P < .05$, $\eta_p^2 = 0.04$) and intensity ($F_{(1,101)} = 15.14$, $P < .01$, $\eta_p^2 = 0.13$). In the right amygdala, we found a main effect of intensity ($F_{(1,101)} = 23.26$, $P < .01$, $\eta_p^2 = 0.17$) and an interaction between emotion and intensity ($F_{(1,101)} = 4.91$, $P = .03$, $\eta_p^2 = 0.05$) but no main effect of treatment or interaction. Consequently, we investigated the effects of dose and latency in the left amygdala.

Effects of latency of oxytocin administration on the left amygdala response to emotional faces

Across three groups of subjects, the latency between administration of OXT (24 IU) or PLC and the start of imaging data acquisition was varied between 15, 45 and 75 min. A repeated measures ANOVA with the within-subject factors emotion intensity, emotional valence, and treatment, the between-subject factor latency of treatment, and the dependent variable left amygdala response revealed main effects of emotion intensity ($F_{(1,64)} = 17.33$, $P < .01$, $\eta_p^2 = 0.21$) and treatment ($F_{(1,64)} = 4.08$, $P < .05$, $\eta_p^2 = 0.06$). Importantly we also observed an interaction between treatment, emotional valence, and latency ($F_{(2,64)} = 3.22$, $P < .05$, $\eta_p^2 = 0.09$). To disentangle this effect, we ran ANOVAs on the response to each stimulus type separately. For high intensity fearful faces, we found a main effect of treatment ($F_{(1,64)} = 4.88$, $P = .031$, $\eta_p^2 = 0.07$), but no main effect of, or interaction with, latency (both P s $> .40$). Post hoc comparisons revealed significant activation decreases 45 min after OXT administration ($t_{(22)} = -2.67$, $P = .01$, $d = 0.92$), but not after 15 or 75 min ($P > .7$ and $P = .25$). For high intensity happy faces, we found an interaction between treatment and latency ($F_{(2,64)} = 4.35$, $P = .02$, $\eta_p^2 = 0.12$), but no main effect of treatment or latency. Post hoc comparisons revealed that the amygdala response to high intensity happy faces was not significantly affected by OXT after 15 or 45 min (respectively: $P > .1$ and $P > .6$), but decreased 75 min after administration ($t_{(19)} = -2.20$, $P = .04$, $d = 0.76$). Importantly, however, this latter effect did not remain significant after Bonferroni correction for multiple comparisons (3 comparisons, $\alpha = 0.05$, revised threshold value of $P = .02$).

No main or interaction effects were found for low intensity faces (both fearful and happy) (see **Supplemental Fig. S5**).

Effects of dose of oxytocin on the left amygdala response to emotional faces

Across three groups of subjects, three doses of OXT (12, 24 and 48 IU) were administered and imaging data were collected 45 min after administration. We conducted a repeated measures ANOVA with the within-subject factors emotion intensity, emotional valence, and treatment, the between-subject factor dose of treatment, and the dependent variable left amygdala responses. Again, as expected, we found a main effect of emotion intensity ($F_{(1,59)} = 4.98, P < .05, \eta_p^2 = 0.08$), but crucially, we also observed a 4-way-interaction between treatment, emotion, intensity and OXT dose ($F_{(2,59)} = 4.17, P < .05, \eta_p^2 = 0.12$). To disentangle this interaction, we ran separate ANOVAs for each stimulus type. For high fearful faces, we found a significant interaction between dose and treatment ($F_{(2,59)} = 4.10, P = .02, \eta_p^2 = 0.12$). This interaction effect was further decomposed by post hoc comparisons, revealing significant activation decreases after 24 IU ($t_{(22)} = -2.67, P = .01, d = 0.92$), but not after 12 IU ($P > .3$). Interestingly, administration of 48 IU of OXT induced a trend-significant activation increase ($t_{(19)} = 1.81, P = .09, d = 0.49$). No main or interaction effects were found with the other stimulus types in these subject groups (see **Supplemental Fig. S6**).

Behavioral results

Task validation

Stimulus variation led to the expected changes in performance: A one-way ANOVA with the recognition rates (categorization task: 'happy', 'neutral' or 'fearful') for the five stimulus conditions obtained under PLC as dependent variable yielded a significant main effect of stimulus condition ($F_{(2,38,254.88)} = 393.91, P < .01, \eta_p^2 = 0.79$). To disentangle this effect, we conducted planned

comparisons, revealing descending hit rates from high happy (mean correct ratings \pm SD = 96 ± 5 %) over high fearful (92 ± 9 %), neutral (90 ± 9 %), low happy (62 ± 21 %) to low fearful faces (39 ± 16 %) (all paired t-tests comparing adjacent face conditions significant with $P < .01$; neutral vs. high fearful faces: $t = 2.05$, $P = 0.043$ i.e. not significant after correction for multiple comparisons). Comparing reaction times (RT) between the different face conditions resulted in a similar pattern (ANOVA main effect: $F_{(3,56,377.11)} = 148.48$, $P < .01$, $\eta_p^2 = 0.58$) and the same order of difficulties (RT high happy (2.27 ± 0.45 s) < high fearful (2.75 ± 0.47 s) < neutral (2.83 ± 0.59 s) < low happy (3.16 ± 0.69 s) < low fearful (3.51 ± 0.72 s), with all paired t-tests but the high fearful vs neutral comparison being significant with $P < .01$).

OXT effects

To examine behavioral effects of OXT treatment, we compared hit rates and response patterns across the five different face categories (neutral, low fearful, high fearful, low happy, high happy) using repeated measures ANOVAS. All analyses were conducted twice, once for the three groups with varying latencies (which all received 24 IU of OXT) and once for the three groups with varying dose of treatment (which were all scanned 45 min after treatment application).

Dose-dependent behavioral OXT effects

A repeated measures ANOVA with the between-subject factor dose (12 IU, 24 IU, 48 IU), the two within-subject factors treatment (OXT, PLC) and stimulus condition (neutral, low fearful, high fearful, low happy, high happy faces) and hit rate as dependent variable revealed neither a main effect of dose ($F_{(2,59)} = 0.376$, $P = .69$, $\eta_p^2 = 0.01$) nor treatment ($F_{(1,59)} = 0.73$, $P = .40$, $\eta_p^2 = 0.01$). As described above, hit rates differed substantially across conditions (main effect of stimulus condition: $F_{(2,32,137.18)} = 278.358$, $P < .001$, $\eta_p^2 = 0.83$). There were no significant interactions.

As expected, recognition rates for high intensity emotional and neutral face stimuli showed strong ceiling effects (> 90 % recognition rate). To uncover dose-dependent OXT effects, we focused on the recognition of ambiguous faces (i.e. low intensity emotional stimuli) as a more sensitive marker of emotion perception. As dependent variable, we chose the proportion of stimuli rated as neutral because this provides a uniform outcome measure for both low intensity happy and low intensity fearful faces. A repeated measures ANOVA with the within-subject factors treatment and emotion (low intensity fearful, low intensity happy) revealed a main effect of emotion ($F_{(1,59)} = 86.96$, $P < .001$, $\eta_p^2 = 0.60$) and treatment ($F_{(1,59)} = 5.21$, $P = .03$, $\eta_p^2 = 0.08$), but no further main or interaction effects. Low intensity fearful faces were more frequently judged as neutral than low intensity happy faces (mean neutral presses fearful faces: 14.00 +/- 0.47 %, happy faces: 8.65 +/- 0.55 %). Irrespective of the emotion, OXT increased the tendency to rate ambiguous faces as neutral (see **Supplemental Fig. S6**, mean neutral presses after OXT: 11.79 +/- 0.45 %, after PLC: 10.86 +/- 0.49 %).

Latency-dependent behavioral OXT effects

Analysis of hit rates across all emotion categories revealed a significant main effect of stimulus condition ($F_{(2,26,140.11)} = 332.70$, $P < .001$, $\eta_p^2 = 0.84$), but no main or interaction effect of treatment ($F_{(1,62)} = 0.108$, $P = .74$, $\eta_p^2 < 0.01$, same ANOVA design as for dose) or latency ($F_{(2,62)} = 0.673$, $P = .51$, $\eta_p^2 = 0.02$).

The analysis of neutral response patterns revealed a main effect of emotion ($F_{(1,62)} = 164.04$, $P < .001$, $\eta_p^2 = 0.73$, same ANOVA design as for dose), with fearful faces being more often recognized as neutral than happy faces (mean neutral presses to fearful faces: 14.10 +/- 0.46 %, happy faces: 8.1 +/- 0.53 %). There was no significant effect of latency on the proportion of trials rated as neutral ($F_{(2,62)} = 0.01$, $P = .91$, $\eta_p^2 < 0.01$), due to very small effects in the 15 and 75 min conditions.

Autism quotient dependent effects

We examined whether autistic-like traits influenced neural responses to each kind of emotional face by conducting regression analyses with AQ as predictor (see **Supplemental Fig. S6**). For high intensity fearful faces [FearHigh_{PLC} > baseline], AQ significantly predicted the neural responses in the right inferior frontal gyrus (peak MNI x, y, z : 58, 18, 8, $t_{(100)} = 5.41$, $k = 44$, $P_{FWE} < .01$) and the left amygdala ($-18, 0, -12$, $t_{(100)} = 5.34$, $k = 55$, $P_{FWE} = .035$; values corrected for multiple comparisons across the whole brain) after PLC treatment. For low intensity fearful faces [FearLow_{PLC} > baseline], AQ significantly correlated with neural responses in the right postcentral gyrus (50, -26, 58, $t_{(100)} = 5.97$, $k = 73$, $P_{FWE} < .01$), the left inferior parietal gyrus ($-42, -26, 38$, $t_{(100)} = 5.61$, $k = 42$, $P_{FWE} = .01$), and the right midcingulate cortex (2, -20, 30, $t_{(100)} = 5.31$ and 18, -8, 52, $k = 228$, $P_{FWE} = .04$). AQ did not predict neural responses to high intensity happy faces in any brain region. For low intensity happy faces [HappyLow_{PLC} > baseline], AQ significantly predicted the neural response in the right midcingulate cortex (2, -16, 30, $t_{(100)} = 6.00$, $k = 71$, $P_{FWE} < .01$) and the right inferior temporal gyrus (52, -20, -20, $t_{(100)} = 5.50$, $k = 41$, $P_{FWE} = .02$).

Importantly, the OXT effect [FearHigh_{OXT} - FearHigh_{PLC}] on amygdala activation was moderated by the AQ. Participants with higher autistic-like traits showed larger OXT effects than participants with lower AQ scores ($R = .23$, $F_{(1,99)} = 5.26$, $P = .02$; regression analysis over all subjects). When looking at the different treatment groups, the moderation was only significant in subjects receiving 24 IU and scanned after 45 min ($R = .51$, $F_{(1,19)} = 6.49$, $P = .02$) with a trend-to-significant effect in the 15 min latency group ($R = .38$, $F_{(1,22)} = 3.65$, $P = .07$). Neither the baseline OXT plasma and saliva concentrations nor the treatment-induced increases were linked to autistic-like traits (all P s > .05).

Further moderation effects

Across subjects, the individual body mass index did neither correlate with the neural ($r = .02$, $P = .86$) nor with the behavioral OXT effect ($r = -.11$, $P = .23$). Likewise, age did not predict neural or

behavioral effects of OXT ($r = .06$, $P = .53$ and $r = .01$, $P = .88$, respectively). Splitting subjects into subsamples of varying dose revealed comparable results, i.e. no moderation effect of body mass index (all P s $> .58$ for neural response, all P s $> .32$ for behavioral response) or age (all P s $> .18$ for neural response, all P s $> .13$ for behavioral response). In no participant group did the administered amount of OXT correlate with the neural or behavioral OXT effects (all P s $> .11$ for neural response, all P s $> .19$ for behavioral response).

Blinding of treatment

Chi-squared tests revealed that the correct guess of treatment in the OXT session did not differ from chance in any of the three dose groups (12 IU: correct estimates 33.3 %; $\chi^2_{(1)} = 3.2$, $P = .07$; 24 IU: correct estimates 40.1 %; $\chi^2_{(1)} = 2.0$, $P = .16$; 48 IU: correct estimates 45.4 %; $\chi^2_{(1)} = 1.8$, $P = .67$). Also, dose groups did not differ in their estimates ($\chi^2_{(2)} = 1.18$, $P = .55$).

SUPPLEMENTAL DISCUSSION

Alternative explanations

Notably, our findings cannot be attributed to unspecific OXT effects on mood or anxiety, as both were measured before and after testing and did not vary with treatment (**Supplemental Table S2**). Moreover, our main findings were based on differential activation in response to fearful compared to neutral faces, which eliminates the influence of OXT on the overall BOLD response or the neural response to faces, effects of individual differences in BOLD signal magnitude, subject-independent variations of the MR signal or other similar confounding effects.

Whole brain findings

Our finding of an increased insula response to emotional stimuli after OXT compared to PLC treatment is in line with previous results: A recent meta-analysis of 11 functional brain imaging studies looking into effects of OXT (17) revealed the left insula as the only region showing a significant OXT-induced augmentation of neural response to emotional stimuli across all studies. Previous findings in regions other than the insula are heterogeneous, but partially corroborate our findings of increased activation following OXT treatment in right cingulate gyrus, right caudate (18), right superior frontal gyrus and left precentral gyrus (19) and decreased activation in right superior temporal sulcus (20) and left medial frontal gyrus (21-23).

Intranasal delivery route

Most recent studies in both human and non-human subjects provide compelling evidence for OXT's central mode of action: Intranasal OXT has been shown to elevate OXT concentrations in the cerebrospinal fluid (CSF) in both macaques (24-26) and humans (27). In particular, Lee and colleagues (26) used a highly sensitive and specific quantitative mass spectrometry assay to distinguish

administered (exogenous) OXT from endogenous OXT in macaques. Measurements of CSF revealed direct penetration by the labeled exogenous OXT into the CSF following both intranasal and intravenous OXT administration. Penetration into the cerebral tissue by intranasal OXT might be much higher than CSF penetration however, because only small amounts of intranasal OXT reach the CSF, where OXT then accumulates over 60-75 min until a detectable signal can be measured (25, 27). Moreover, a recent study in mice indicates that intranasal OXT quickly permeates into specific brain areas (28), thus providing further evidence for OXT's central mode of action (29) and the utility of intranasal OXT administration as a pharmacological tool to modulate central OXT availability. More generally, a plethora of human studies has further underlined the effect of intranasal OXT on various forms of higher order interpersonal behaviors such as cooperation (30), trust (31, 32), and romantic relationships (33-35).

SUPPLEMENTAL TABLES

Table S1. Demographics and psychological screening

	24 IU 15 min (n = 24)	24 IU 45 min (n = 25)	24 IU 75 min (n = 24)	12 IU 45 min (n = 20)	48 IU 45 min (n = 22)	<i>F</i>	<i>P</i>
Age (y)	23.9 (3.3)	24.9 (4.2)	24.9 (4.9)	25.5 (5.2)	24.6 (4.3)	0.34	.85
Educ. (y)	17.0 (2.6)	16.9 (2.6)	16.4 (3.4)	17.7 (3.3)	17.2 (3.0)	0.49	.75
AQ¹	14.9 (5.9)	15.3 (4.6)	13.6 (4.7)	13.2 (4.1)	13.6 (5.2)	0.74	.57
TAS²	47.7 (5.5)	51.8 (10.6)	48.7 (6.8)	47.5 (5.1)	48.0 (8.5)	1.23	.30
BDI³	1.9 (2.5)	1.5 (1.6)	2.1 (2.2)	3.6 (4.0)	2.2 (3.2)	1.58	.19
STAI⁴	30.6 (6.3)	31.2 (5.1)	33.2 (5.9)	33.0 (6.3)	30.1 (7.2)	1.10	.36
TMT-A⁵ (s)	20.6 (4.2)	21.1 (5.1)	25.0 (6.7)	23.0 (7.7)	21.3 (8.2)	1.71	.15
TMT-B⁵(s)	54.0 (19.7)	57.4 (18.9)	61.7 (19.2)	55.8 (15.3)	58.1 (17.8)	0.54	.71
MWTA⁶	31.8 (2.5)	31.5 (3.2)	32.1 (2.4)	31.7 (2.1)	32.1 (2.9)	0.20	.93
LPS4⁷	32.3 (3.9)	30.9 (4.5)	31.3 (3.5)	29.7 (3.7)	30.6 (3.5)	1.26	.29
Digit Span sum⁸	16.3 (2.9)	17.4 (3.8)	18.7 (4.5)	17.7 (4.0)	17.1 (3.8)	1.16	.33

Notes. Values are means and SD. Educ. = Education. ¹ Autistic-like traits were measured with the Autism-Spectrum Quotient, AQ. ² Alexithymia was measured with the Toronto Alexithymia Scale, TAS. ³ Depressive symptoms were measured with the Beck Depression Inventory, Version II, BDI. ⁴ Trait anxiety was measured with the State-Trait Anxiety Inventory, STAI. ⁵ Visual attention and task-switching were assessed using the TMT-A and TMT-B (Trail-making test A, B). ⁶ Verbal IQ based on lexical decisions was assessed by the MWT-A (Mehrfachwahl-Wortschatz-Intelligenz-Test Teil A) (maximum possible score 37). ⁷ Nonverbal reasoning IQ was assessed by the LPS (Leistungspruefssystem) subtest 4 (maximum possible score 40). ⁸ Working memory performance was assessed using the digit span forward and backward test (sum is given, maximum possible score 28).

Table S2. Measurements of anxiety and mood

	PLC session		OXT session		F_{treat}	P	$F_{treat*time}$	P
	pre	post	pre	post				
STAI^a	34.3 (5.1)	32.8 (6.2)	33.3 (5.1)	32.7 (5.7)	1.21	.27	1.8	.18
PANAS								
- pos ^b	30.1 (6.3)	29.5 (6.6)	30.4 (5.3)	29.4 (6.9)	0.8	.77	0.38	.54
- neg ^b	11.9 (3.1)	11.2 (2.2)	11.6 (2.3)	11.0 (2.0)	1.7	.19	0.75	.39

Notes. Values are means and SD. State anxiety before and after the experiment was assessed using the
^a STAI = State-Trait Anxiety Inventory. Mood before and after the experiment was assessed using the
^b PANAS = Positive and Negative Affect Schedule. Abbreviations: neg, negative affect; OXT, oxytocin; PLC, placebo; pos, positive affect; time: pre and post; treat, treatment: OXT and PLC.

Table S3. Whole brain findings under PLC (thresholded at $P_{FWE} < .01$)

Region	Right/left	Cluster size (voxels)	t-score $t_{(808)}$	MNI coordinates		
				x	y	z
T-test emotional faces > neutral faces						
Inferior frontal gyrus (operculum)	R	3649	9.61	54	16	28
Inferior frontal gyrus (triangular)	L	3483	9.41	-50	16	-4
Inferior parietal lobule gyrus	R	8077	8.13	38	-44	42
Midcingulate gyrus	R	425	7.73	-2	-22	28
Pallidum	R	451	6.46	10	0	2
Superior medial frontal gyrus	L	1386	6.32	-4	26	46

Notes. Abbreviations: FWE, family-wise error corrected; L, left; MNI, Montreal Neurological Institute; PLC, placebo; R, right.

Table S4. Whole brain OXT effects (thresholded at $P_{FWE} < .05$)

Region	Right/left	Cluster size (voxels)	t-score $t_{(808)}$	MNI coordinates		
				x	y	z
T-test OXT > PLC						
[emotional faces > neutral faces]						
Insula	R	140	5.68	30	-22	20
Insula	L	87	5.40	-32	14	-12
Cingulate cortex	R	36	5.34	10	-2	46
Caudatus	R	52	5.24	16	12	8
Superior frontal gyrus	R	81	5.20	18	52	30
Precentral gyrus	L	31	4.94	-38	-12	60
T-test OXT < PLC						
[emotional faces > neutral faces]						
Superior temporal sulcus	R	42	5.10	48	-12	0
Superior medial frontal gyrus	L	41	5.07	-6	28	46

Notes. Abbreviations: FWE, family-wise error corrected; L, left; MNI, Montreal Neurological Institute; OXT, oxytocin; PLC, placebo; R, right.

SUPPLEMENTAL FIGURES



Figure S1: Series of morphed facial expressions; transition from neutral to fearful expression in change increments of 5 %. Black frames indicate the full expressions, as originally derived from the KDEF (image identifier: 'AF02NES.JPG' and 'AF02AFS.JPG'). Blue frames indicate the face pictures showing 35 % and 65 % intensity of fear, which were chosen for the final stimulus pool as pictures of low and high fear, respectively.

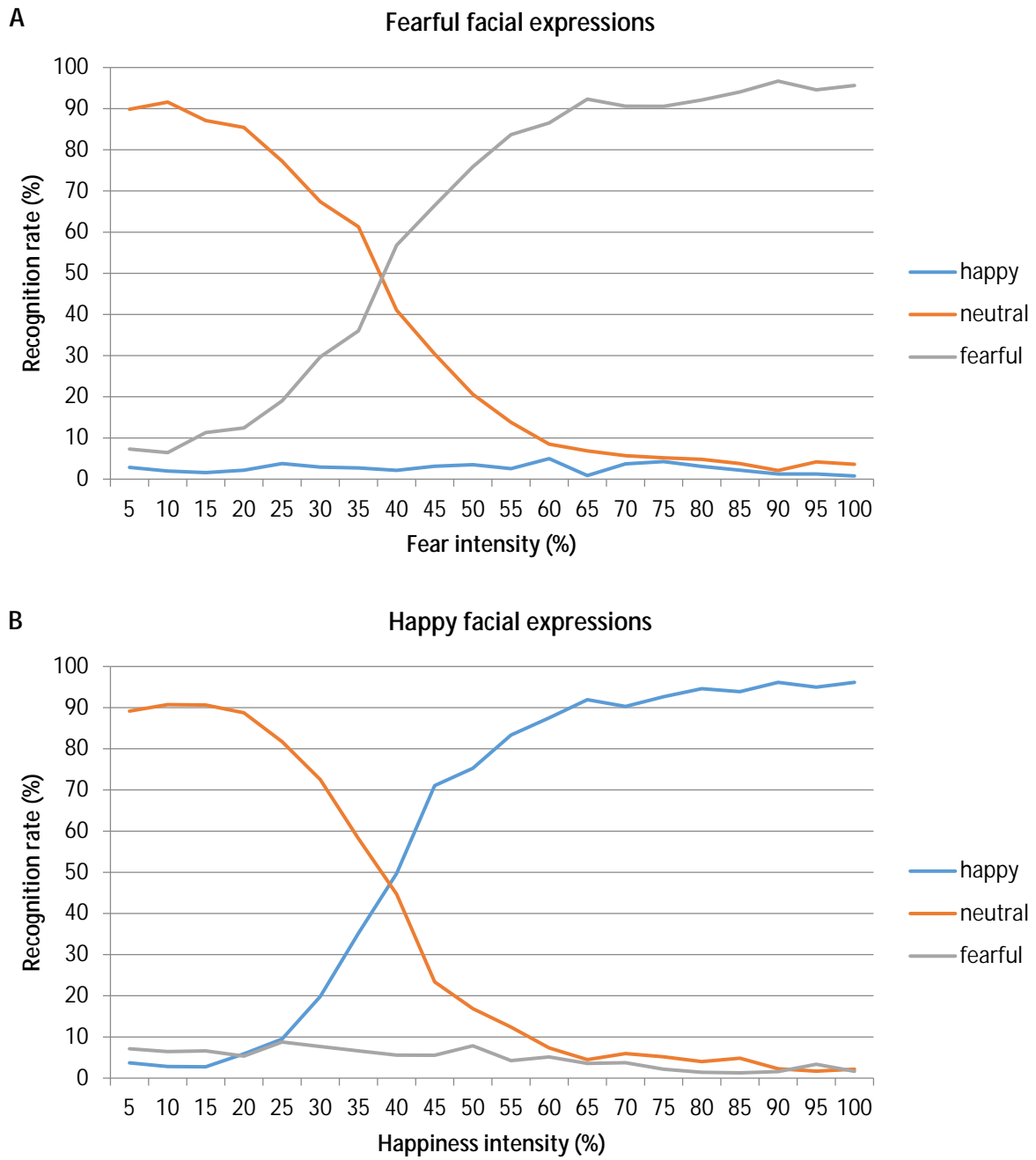


Figure S2: Recognition rates as a function of emotion intensity. In a pilot study, participants were asked to rate the expressions as happy (blue), neutral (orange), or fearful (gray). In **A**, ratings of increasingly fearful expression are shown. In **B**, ratings of increasingly happy expressions are shown. An emotional intensity of 0 equals neutral mood, an intensity of 100 equals full emotional expression.

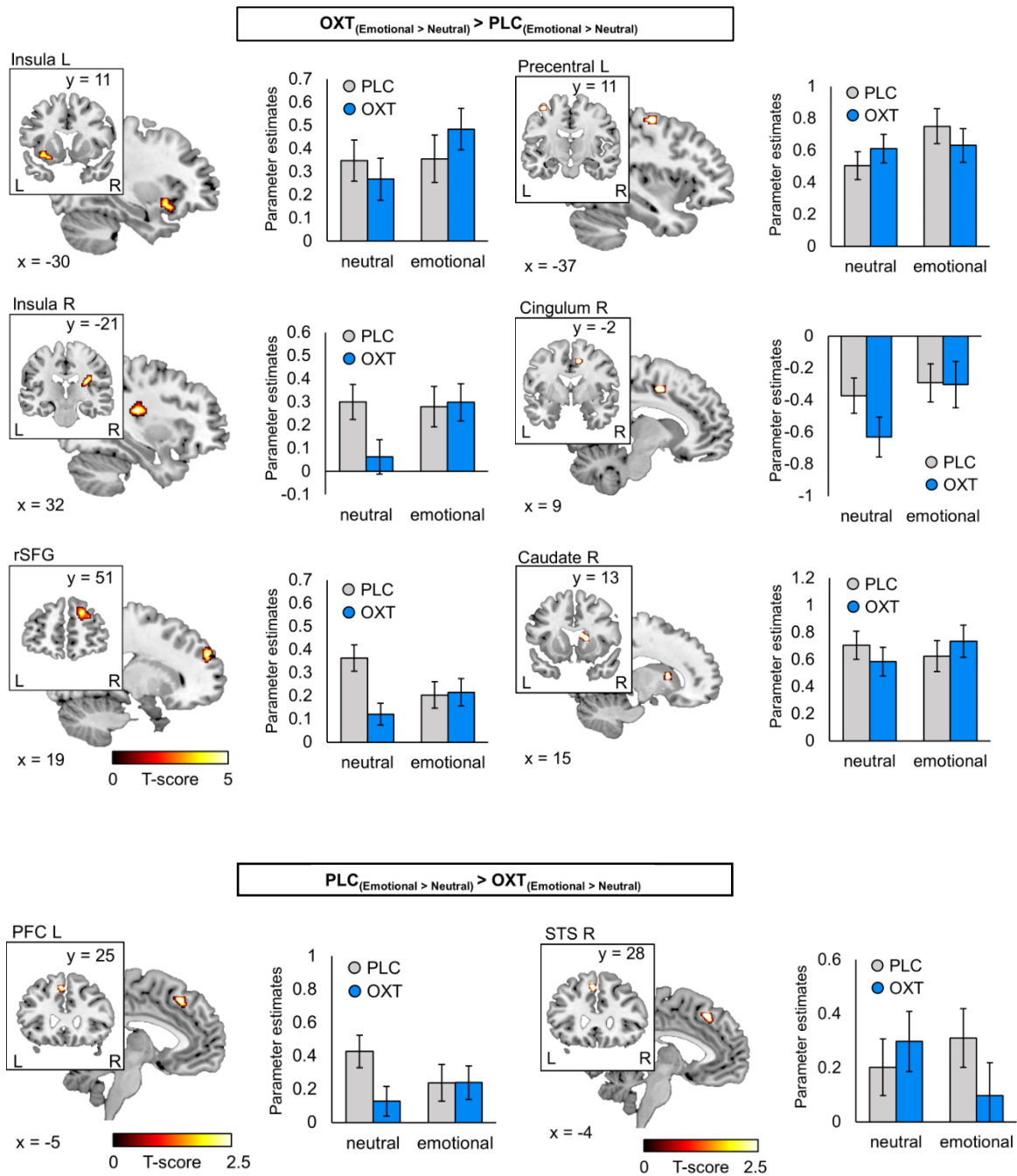


Figure S3: OXT effects on neural response to emotional vs neutral faces. For each cluster with significant whole brain activation at $P < .05$ (family-wise error corrected at peak level) parameter estimates are given in the corresponding bar chart (arbitrary unit). Error bars indicate standard error of the mean. Abbreviations: L, left hemisphere; OXT, oxytocin; PFC, prefrontal cortex; PLC, placebo, R, right hemisphere; rSFG, right superior frontal gyrus; STS, superior temporal sulcus.

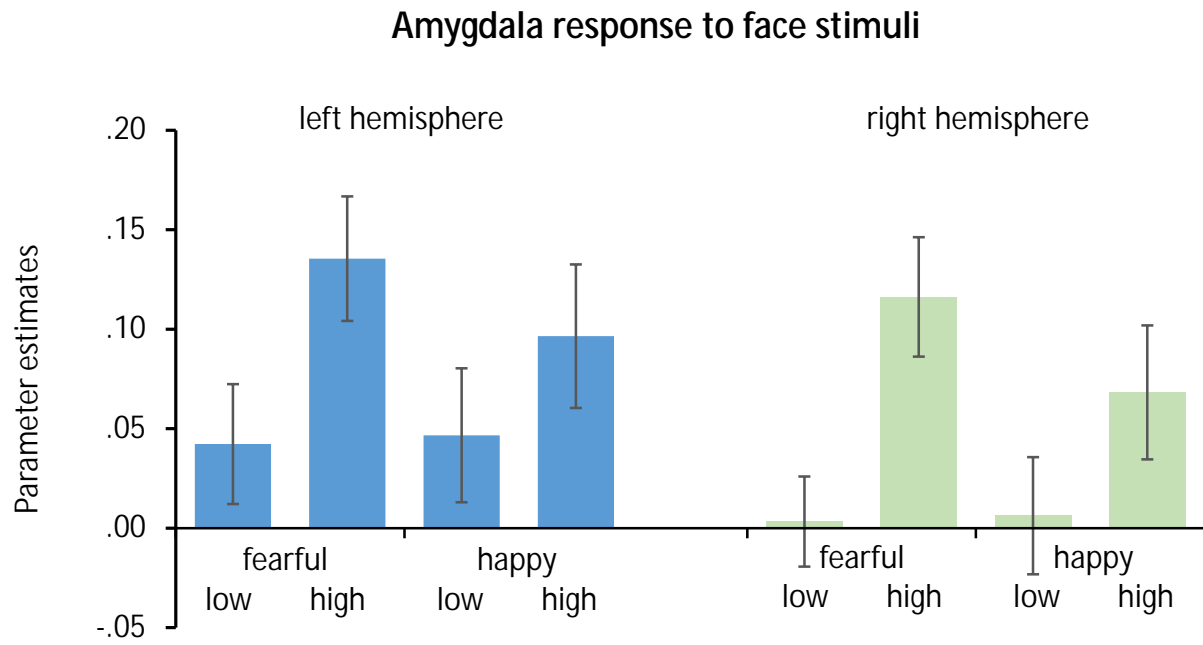


Figure S4: Amygdala response to emotional face stimuli minus the response to neutral faces (all under PLC), given as parameter estimates (arbitrary unit). Error bars indicate standard error of the mean.

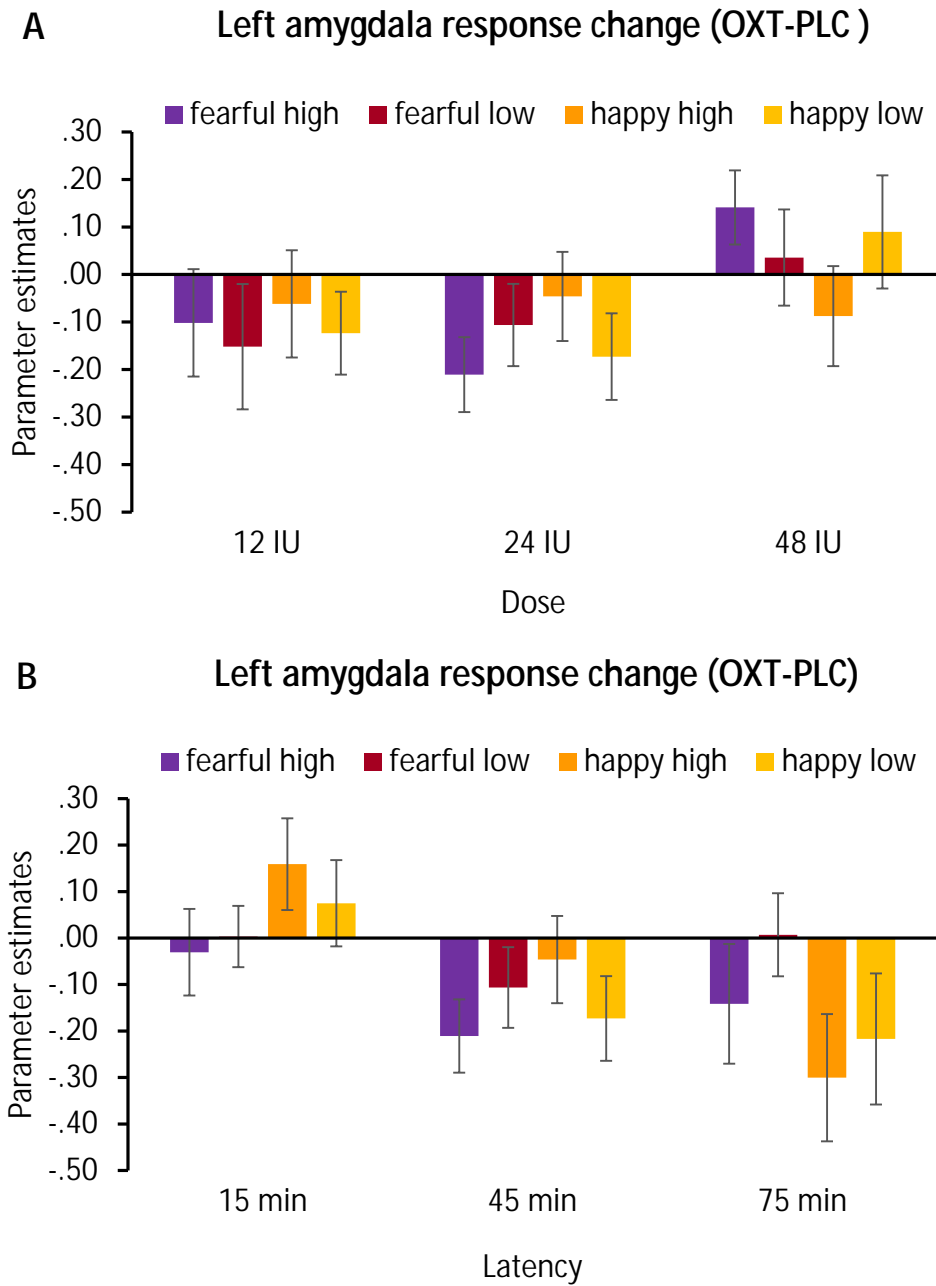


Figure S5: OXT effect on left amygdala response to emotional face stimuli normalized by response to neutral faces. Each treatment dose (A) and latency (B) condition is shown separately. Difference values (OXT-PLC) are given as parameter estimates (arbitrary unit). Error bars indicate standard error of the mean. Abbreviations: IU, international units; min, minutes; OXT, oxytocin; PLC, placebo.

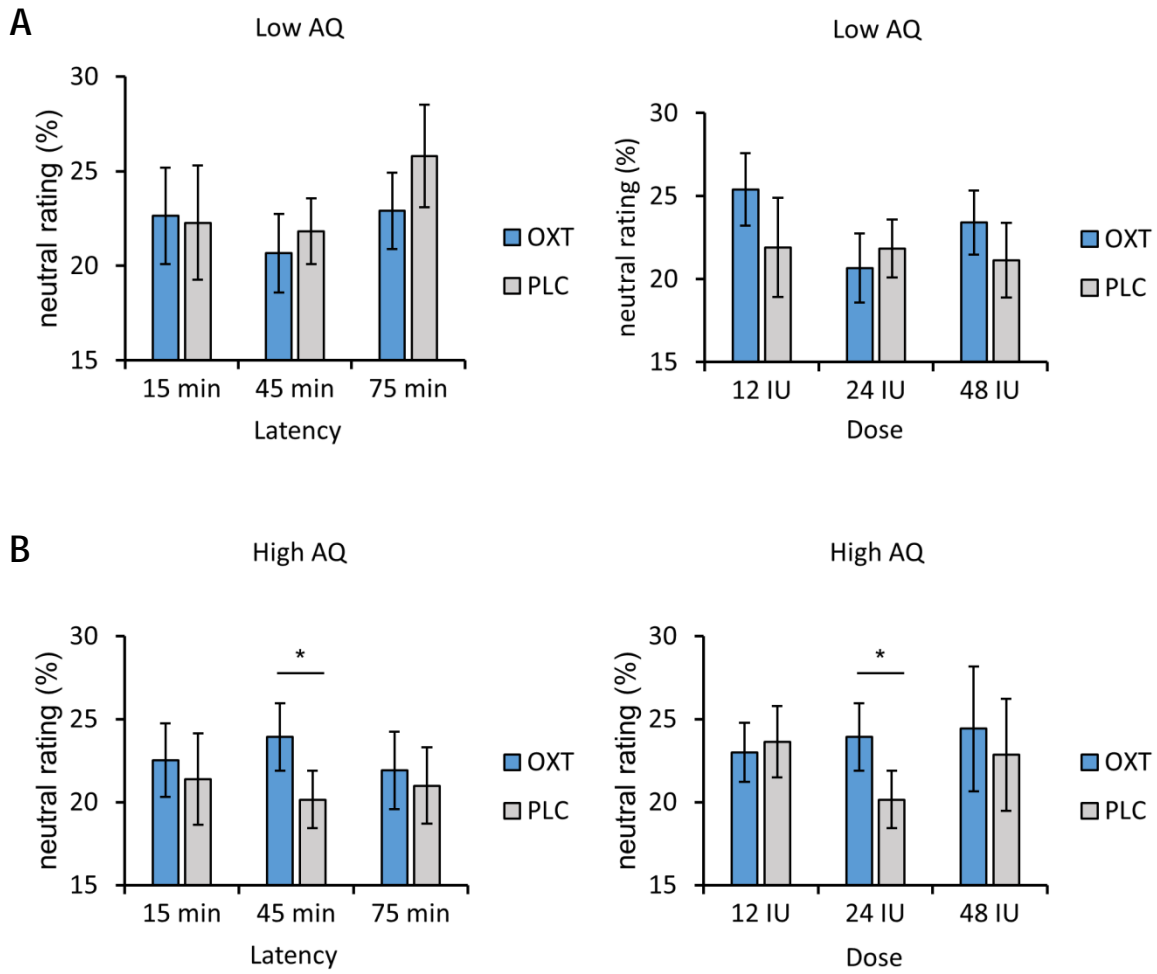


Figure S6: OXT effect on the rating of ambiguous faces (i.e. low intense happy and fearful faces) in subjects with low (A) and high (B) autistic-like traits. Values depict the percentage of trials in which the subjects rated an ambiguous face as neutral. Error bars indicate standard error of the mean. Abbreviations: AQ, autism quotient; IU, international units; min, minutes; OXT, oxytocin; PLC, placebo.

SUPPLEMENTAL REFERENCES

1. Sheehan DV, Lecrubier Y, Sheehan KH, Amorim P, Janavs J, Weiller E, et al. (1998): The Mini-International Neuropsychiatric Interview (MINI): the development and validation of a structured diagnostic psychiatric interview for DSM-IV and ICD-10. *J Clin Psychiatry*.
2. Spielberger CD (1983): Manual for the State-Trait Anxiety Inventory STAI.
3. Beck AT, Steer RA, Brown GK (1996): *Beck depression inventory-II*. San Antonio, TX: Psychological Corporation.
4. Taylor GJ, Bagby RM, Parker JD (2003): The 20-Item Toronto Alexithymia Scale: IV. Reliability and factorial validity in different languages and cultures. *J Psychosom Res*. 55:277-283.
5. Baron-Cohen S, Wheelwright S, Skinner R, Martin J, Clubley E (2001): The autism-spectrum quotient (AQ): Evidence from asperger syndrome/high-functioning autism, males and females, scientists and mathematicians. *J Autism Dev Disord*. 31:5-17.
6. Kagerbauer SM, Martin J, Schuster T, Blobner M, Kochs EF, Landgraf R (2013): Plasma oxytocin and vasopressin do not predict neuropeptide concentrations in human cerebrospinal fluid. *J Neuroendocrinol*. 25:668-673.
7. Shahrestani S, Kemp AH, Guastella AJ (2013): The impact of a single administration of intranasal oxytocin on the recognition of basic emotions in humans: a meta-analysis. *Neuropsychopharmacology*. 38:1929-1936.
8. Lundqvist D, Flykt A, Ohman A (1998): Karolinska Directed Emotional Faces. Nature Publishing Group.
9. Stocker T, Kellermann T, Schneider F, Habel U, Amunts K, Pieperhoff P, et al. (2006): Dependence of amygdala activation on echo time: results from olfactory fMRI experiments. *Neuroimage*. 30:151-159.
10. Evans AC, Marrett S, Neelin P, Collins L, Worsley K, Dai W, et al. (1992): Anatomical mapping of functional activation in stereotactic coordinate space. *Neuroimage*. 1:43-53.
11. Holmes CJ, Hoge R, Collins L, Woods R, Toga AW, Evans AC (1998): Enhancement of MR images using registration for signal averaging. *J Comput Assist Tomogr*. 22:324-333.
12. Maldjian JA, Laurienti PJ, Kraft RA, Burdette JH (2003): An automated method for neuroanatomic and cytoarchitectonic atlas-based interrogation of fMRI data sets. *Neuroimage*. 19:1233-1239.
13. Kriegeskorte N, Simmons WK, Bellgowan PS, Baker CI (2009): Circular analysis in systems neuroscience: the dangers of double dipping. *Nat Neurosci*. 12:535-540.
14. Judd CM, Kenny DA, McClelland GH (2001): Estimating and testing mediation and moderation in within-subject designs. *Psychol Methods*. 6:115-134.
15. Eickhoff SB, Stephan KE, Mohlberg H, Grefkes C, Fink GR, Amunts K, et al. (2005): A new SPM toolbox for combining probabilistic cytoarchitectonic maps and functional imaging data. *Neuroimage*. 25:1325-1335.
16. Fusar-Poli P, Placentino A, Carletti F, Landi P, Allen P, Surguladze S, et al. (2009): Functional atlas of emotional faces processing: a voxel-based meta-analysis of 105 functional magnetic resonance imaging studies. *J Psychiatry Neurosci*. 34:418-432.
17. Wigton R, Radua J, Allen P, Averbach B, Meyer-Lindenberg A, McGuire P, et al. (2015): Neurophysiological effects of acute oxytocin administration: systematic review and meta-analysis of placebo-controlled imaging studies. *J Psychiatry Neurosci*. 40:E1-22.

18. Pincus D, Kose S, Arana A, Johnson K, Morgan PS, Borckardt J, et al. (2010): Inverse effects of oxytocin on attributing mental activity to others in depressed and healthy subjects: a double-blind placebo controlled fMRI study. *Front Psychiatry*. 1:134.
19. Domes G, Lischke A, Berger C, Grossmann A, Hauenstein K, Heinrichs M, et al. (2010): Effects of intranasal oxytocin on emotional face processing in women. *Psychoneuroendocrinology*. 35:83-93.
20. Wittfoth-Schardt D, Grunding J, Wittfoth M, Lanfermann H, Heinrichs M, Domes G, et al. (2012): Oxytocin modulates neural reactivity to children's faces as a function of social salience. *Neuropsychopharmacology*. 37:1799-1807.
21. Labuschagne I, Phan KL, Wood A, Angstadt M, Chua P, Heinrichs M, et al. (2011): Medial frontal hyperactivity to sad faces in generalized social anxiety disorder and modulation by oxytocin. *Int J Neuropsychopharmacol*. 1-14.
22. Domes G, Heinrichs M, Gläscher J, Büchel C, Braus DF, Herpertz SC (2007): Oxytocin attenuates amygdala responses to emotional faces regardless of valence. *Biol Psychiatry*. 62:1187-1190.
23. Petrovic P, Kalisch R, Singer T, Dolan RJ (2008): Oxytocin attenuates affective evaluations of conditioned faces and amygdala activity. *J Neurosci*. 28:6607-6615.
24. Dal Monte O, Noble PL, Turchi J, Cummins A, Averbeck BB (2014): CSF and blood oxytocin concentration changes following intranasal delivery in macaque. *PLoS One*. 9.
25. Lee M (2016): Direct Evidence of Cerebrospinal Fluid Penetration of Oxytocin After Intranasal and Intravenous Administration and Effect of Systemic Oxytocin Administration on Methylphenidate-Induced Changes in Accumbal Dopamine Levels and Methylphenidate Self-Administration; ACNP 55th Annual Meeting. *Neuropsychopharmacology*. 41:S1-S115.
26. Lee MR, Scheidweiler KB, Diao XX, Akhlaghi F, Cummins A, Huestis MA, et al. (2017): Oxytocin by intranasal and intravenous routes reaches the cerebrospinal fluid in rhesus macaques: determination using a novel oxytocin assay. *Mol Psychiatry*.
27. Striepens N, Kendrick KM, Hanking V, Landgraf R, Wullner U, Maier W, et al. (2013): Elevated cerebrospinal fluid and blood concentrations of oxytocin following its intranasal administration in humans. *Sci Rep*. 3:3440.:10.1038/srep03440.
28. Smith, A. S., Korgan, A. C., Fastman, J., Granovetter, M. C., Song, J., Young, W. S. (2016) Nasal oxytocin in a genetic knockout: Pharmacokinetics and behavior. Poster presented at the *Society for Neuroscience conference* in San Diego, CA
29. Kanat M, Heinrichs M, Domes G (2014): Oxytocin and the social brain: neural mechanisms and perspectives in human research. *Brain Res*. 11:160-171.
30. Declerck CH, Boone C, Kiyonari T (2014): The effect of oxytocin on cooperation in a prisoner's dilemma depends on the social context and a person's social value orientation. *Soc Cogn Affect Neurosci*. 9:802-809.
31. Kosfeld M, Heinrichs M, Zak PJ, Fischbacher U, Fehr E (2005): Oxytocin increases trust in humans. *Nature*. 435:673-676.
32. Baumgartner T, Heinrichs M, Vonlanthen A, Fischbacher U, Fehr E (2008): Oxytocin shapes the neural circuitry of trust and trust adaptation in humans. *Neuron*. 58:639-650.
33. Scheele D, Striepens N, Gunturkun O, Deutschlander S, Maier W, Kendrick KM, et al. (2012): Oxytocin modulates social distance between males and females. *J Neurosci*. 32:16074-16079.
34. Scheele D, Wille A, Kendrick KM, Stoffel-Wagner B, Becker B, Gunturkun O, et al. (2013): Oxytocin enhances brain reward system responses in men viewing the face of their female partner. *Proc Natl Acad Sci U S A*. 110:20308-20313.

35. Hurlemann R, Scheele D (2016): Dissecting the Role of Oxytocin in the Formation and Loss of Social Relationships. *Biol Psychiatry*. 79:185-193.



CONSORT 2010 checklist of information to include when reporting a randomised trial*

Section/Topic	Item No	Checklist item	Reported on page No
Title and abstract			
	1a	Identification as a randomised trial in the title	<u>2</u>
	1b	Structured summary of trial design, methods, results, and CONCLUSIONS (for specific guidance see CONSORT for abstracts)	<u>2</u>
Introduction			
Background and objectives			
	2a	Scientific background and explanation of rationale	<u>3-4</u>
	2b	Specific objectives or hypotheses	<u>4</u>
Methods			
Trial design			
	3a	Description of trial design (such as parallel, factorial) including allocation ratio	<u>5</u>
	3b	Important changes to methods after trial commencement (such as eligibility criteria), with reasons	<u>n.a.</u>
Participants			
	4a	Eligibility criteria for participants	<u>5, SI-Methods</u>
	4b	Settings and locations where the data were collected	<u>5</u>
Interventions			
	5	The interventions for each group with sufficient details to allow replication, including how and when they were actually administered	<u>6</u>
Outcomes			
	6a	Completely defined pre-specified primary and secondary outcome measures, including how and when they were assessed	<u>5-7</u>
	6b	Any changes to trial outcomes after the trial commenced, with reasons	<u>n.a.</u>
Sample size			
	7a	How sample size was determined	<u>5</u>
	7b	When applicable, explanation of any interim analyses and stopping guidelines	<u>-</u>
Randomisation:			
Sequence generation			
	8a	Method used to generate the random allocation sequence	<u>5</u>
	8b	Type of randomisation; details of any restriction (such as blocking and block size)	<u>5</u>
Allocation concealment mechanism			
	9	Mechanism used to implement the random allocation sequence (such as sequentially numbered containers), describing any steps taken to conceal the sequence until interventions were assigned	<u>5</u>
Implementation			
	10	Who generated the random allocation sequence, who enrolled participants, and who assigned participants to interventions	<u>16</u>
Blinding			
	11a	If done, who was blinded after assignment to interventions (for example, participants, care providers, those	<u>5</u>

		assessing outcomes) and how	
	11b	If relevant, description of the similarity of interventions	6-7, SI- Methods
Statistical methods	12a	Statistical methods used to compare groups for primary and secondary outcomes	6-7, SI- Methods
	12b	Methods for additional analyses, such as subgroup analyses and adjusted analyses	6-7, SI- Methods
Results			
Participant flow (a diagram is strongly recommended)	13a	For each group, the numbers of participants who were randomly assigned, received intended treatment, and were analysed for the primary outcome	5, SI-Flow Diagram
	13b	For each group, losses and exclusions after randomisation, together with reasons	SI-Methods
Recruitment	14a	Dates defining the periods of recruitment and follow-up	SI-Methods
	14b	Why the trial ended or was stopped	-
Baseline data	15	A table showing baseline demographic and clinical characteristics for each group	SI-Results
Numbers analysed	16	For each group, number of participants (denominator) included in each analysis and whether the analysis was by original assigned groups	8-11, SI-Results
Outcomes and estimation	17a	For each primary and secondary outcome, results for each group, and the estimated effect size and its precision (such as 95% confidence interval)	8-11
	17b	For binary outcomes, presentation of both absolute and relative effect sizes is recommended	
Ancillary analyses	18	Results of any other analyses performed, including subgroup analyses and adjusted analyses, distinguishing pre-specified from exploratory	SI-Results
Harms	19	All important harms or unintended effects in each group (for specific guidance see CONSORT for harms)	-
Discussion			
Limitations	20	Trial limitations, addressing sources of potential bias, imprecision, and, if relevant, multiplicity of analyses	12-15
Generalisability	21	Generalisability (external validity, applicability) of the trial findings	12-15
Interpretation	22	Interpretation consistent with results, balancing benefits and harms, and considering other relevant evidence	12-15
Other information			
Registration	23	Registration number and name of trial registry	SI-Methods
Protocol	24	Where the full trial protocol can be accessed, if available	
Funding	25	Sources of funding and other support (such as supply of drugs), role of funders	16



Flow Diagram

